ISSN 1726-5749

SENSORS & TRANSDUCERS

8 vol. 6 Special /09

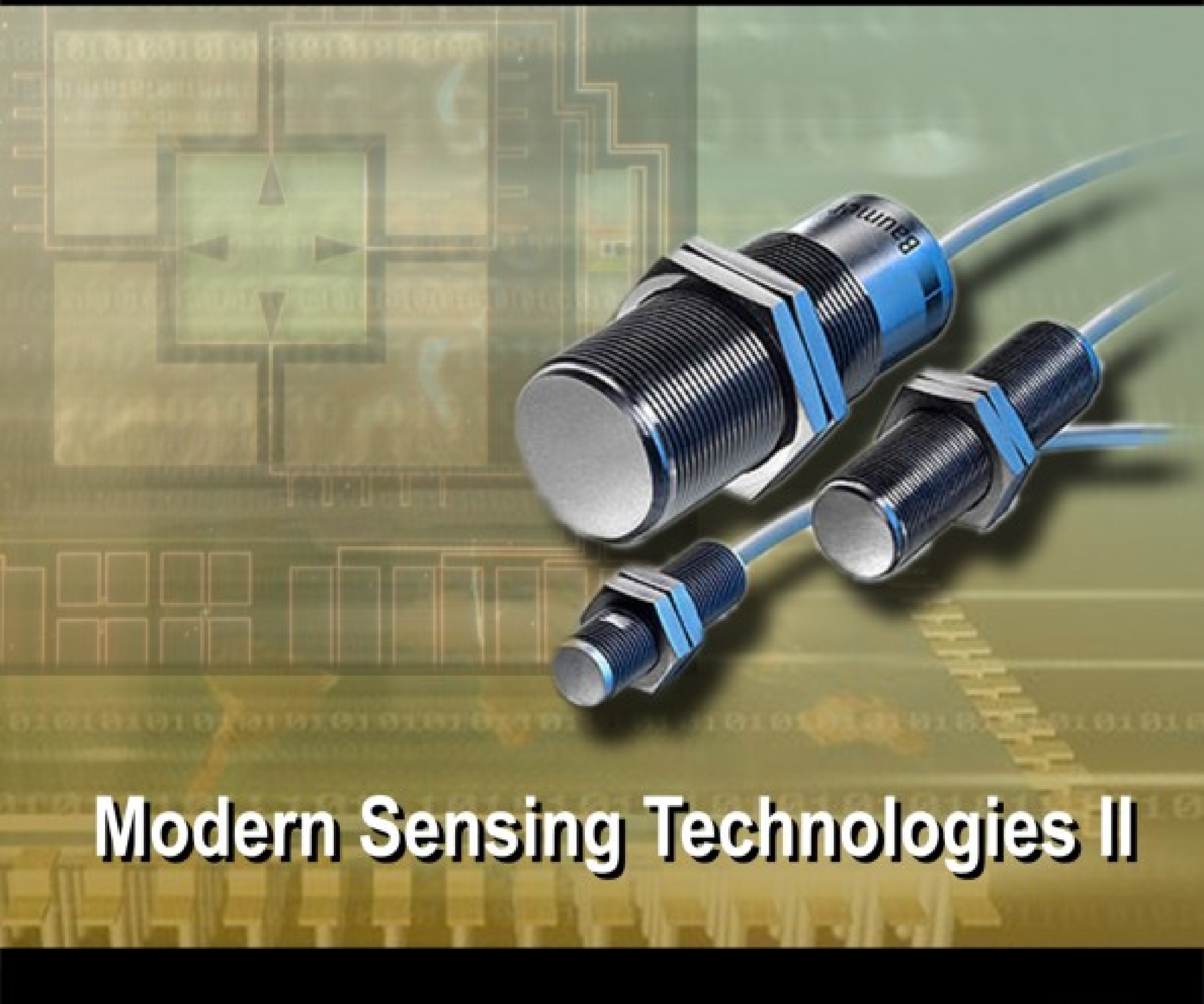

Modern Sensing Technologies II

International Frequency Sensor Association Publishing

IFSA

Sensors & Transducers

Volume 6, Special Issue
August 2009
www.sensorsportal.com
ISSN 1726-5479

Editors-in-Chief: professor Sergey Y. Yurish, phone: +34 696067716, fax: +34 93 4011989, e-mail: editor@sensorsportal.com
Guest Editors: Subhas Chandra Mukhopadhyay, Gourab Sen Gupta and Ray Yueh Min Huang

Editors for Western Europe
Meijer, Gerard C.M., Delft University of Technology, The Netherlands
Ferrari, Vittorio, Universitá di Brescia, Italy

Editor South America
Costa-Felix, Rodrigo, Inmetro, Brazil

Editor for Eastern Europe
Sachenko, Anatoly, Ternopil State Economic University, Ukraine

Editors for North America
Datskos, Panos G., Oak Ridge National Laboratory, USA
Fabien, J. Josse, Marquette University, USA
Katz, Evgeny, Clarkson University, USA

Editor for Asia
Ohyama, Shinji, Tokyo Institute of Technology, Japan

Editor for Asia-Pacific
Mukhopadhyay, Subhas, Massey University, New Zealand

Editorial Advisory Board

Abdul Rahim, Ruzairi, Universiti Teknologi, Malaysia
Ahmad, Mohd Noor, Nothern University of Engineering, Malaysia
Annamalai, Karthigeyan, National Institute of Advanced Industrial Science and Technology, Japan
Arcega, Francisco, University of Zaragoza, Spain
Arguel, Philippe, CNRS, France
Ahn, Jae-Pyoung, Korea Institute of Science and Technology, Korea
Arndt, Michael, Robert Bosch GmbH, Germany
Ascoli, Giorgio, George Mason University, USA
Atalay, Selcuk, Inonu University, Turkey
Atghiaee, Ahmad, University of Tehran, Iran
Augutis, Vygantas, Kaunas University of Technology, Lithuania
Avachit, Patil Lalchand, North Maharashtra University, India
Ayesh, Aladdin, De Montfort University, UK
Bahreyni, Behraad, University of Manitoba, Canada
Baliga, Shankar, B., General Monitors Transnational, USA
Baoxian, Ye, Zhengzhou University, China
Barford, Lee, Agilent Laboratories, USA
Barlingay, Ravindra, RF Arrays Systems, India
Basu, Sukumar, Jadavpur University, India
Beck, Stephen, University of Sheffield, UK
Ben Bouzid, Sihem, Institut National de Recherche Scientifique, Tunisia
Benachaiba, Chellali, Universitaire de Bechar, Algeria
Binnie, T. David, Napier University, UK
Bischoff, Gerlinde, Inst. Analytical Chemistry, Germany
Bodas, Dhananjay, IMTEK, Germany
Borges Carval, Nuno, Universidade de Aveiro, Portugal
Bousbia-Salah, Mounir, University of Annaba, Algeria
Bouvet, Marcel, CNRS – UPMC, France
Brudzewski, Kazimierz, Warsaw University of Technology, Poland
Cai, Chenxin, Nanjing Normal University, China
Cai, Qingyun, Hunan University, China
Campanella, Luigi, University La Sapienza, Italy
Carvalho, Vitor, Minho University, Portugal
Cecelja, Franjo, Brunel University, London, UK
Cerda Belmonte, Judith, Imperial College London, UK
Chakrabarty, Chandan Kumar, Universiti Tenaga Nasional, Malaysia
Chakravorty, Dipankar, Association for the Cultivation of Science, India
Changhai, Ru, Harbin Engineering University, China
Chaudhari, Gajanan, Shri Shivaji Science College, India
Chavali, Murthy, VIT University, Tamil Nadu, India
Chen, Jiming, Zhejiang University, China
Chen, Rongshun, National Tsing Hua University, Taiwan
Cheng, Kuo-Sheng, National Cheng Kung University, Taiwan
Chiang, Jeffrey (Cheng-Ta), Industrial Technol. Research Institute, Taiwan
Chiriac, Horia, National Institute of Research and Development, Romania
Chowdhuri, Arijit, University of Delhi, India
Chung, Wen-Yaw, Chung Yuan Christian University, Taiwan
Corres, Jesus, Universidad Publica de Navarra, Spain
Cortes, Camilo A., Universidad Nacional de Colombia, Colombia
Courtois, Christian, Universite de Valenciennes, France
Cusano, Andrea, University of Sannio, Italy
D'Amico, Arnaldo, Università di Tor Vergata, Italy
De Stefano, Luca, Institute for Microelectronics and Microsystem, Italy
Deshmukh, Kiran, Shri Shivaji Mahavidyalaya, Barshi, India
Dickert, Franz L., Vienna University, Austria
Dieguez, Angel, University of Barcelona, Spain
Dimitropoulos, Panos, University of Thessaly, Greece
Ding, Jianning, Jiangsu Polytechnic University, China
Djordjevich, Alexandar, City University of Hong Kong, Hong Kong
Donato, Nicola, University of Messina, Italy
Donato, Patricio, Universidad de Mar del Plata, Argentina
Dong, Feng, Tianjin University, China
Drljaca, Predrag, Instersema Sensoric SA, Switzerland
Dubey, Venketesh, Bournemouth University, UK
Enderle, Stefan, Univ.of Ulm and KTB Mechatronics GmbH, Germany
Erdem, Gursan K. Arzum, Ege University, Turkey
Erkmen, Aydan M., Middle East Technical University, Turkey
Estelle, Patrice, Insa Rennes, France
Estrada, Horacio, University of North Carolina, USA
Faiz, Adil, INSA Lyon, France
Fericean, Sorin, Balluff GmbH, Germany
Fernandes, Joana M., University of Porto, Portugal
Francioso, Luca, CNR-IMM Institute for Microelectronics and Microsystems, Italy
Francis, Laurent, University Catholique de Louvain, Belgium
Fu, Weiling, South-Western Hospital, Chongqing, China
Gaura, Elena, Coventry University, UK
Geng, Yanfeng, China University of Petroleum, China
Gole, James, Georgia Institute of Technology, USA
Gong, Hao, National University of Singapore, Singapore
Gonzalez de la Rosa, Juan Jose, University of Cadiz, Spain
Granel, Annette, Goteborg University, Sweden
Graff, Mason, The University of Texas at Arlington, USA
Guan, Shan, Eastman Kodak, USA
Guillet, Bruno, University of Caen, France
Guo, Zhen, New Jersey Institute of Technology, USA
Gupta, Narendra Kumar, Napier University, UK
Hadjiloucas, Sillas, The University of Reading, UK
Haider, Mohammad R., Sonoma State University, USA
Hashsham, Syed, Michigan State University, USA
Hasni, Abdelhafid, Bechar University, Algeria
Hernandez, Alvaro, University of Alcala, Spain
Hernandez, Wilmar, Universidad Politecnica de Madrid, Spain
Homentcovschi, Dorel, SUNY Binghamton, USA
Horstman, Tom, U.S. Automation Group, LLC, USA
Hsiai, Tzung (John), University of Southern California, USA
Huang, Jeng-Sheng, Chung Yuan Christian University, Taiwan
Huang, Star, National Tsing Hua University, Taiwan
Huang, Wei, PSG Design Center, USA
Hui, David, University of New Orleans, USA
Jaffrezic-Renault, Nicole, Ecole Centrale de Lyon, France
Jaime Calvo-Galleg, Jaime, Universidad de Salamanca, Spain
James, Daniel, Griffith University, Australia
Janting, Jakob, DELTA Danish Electronics, Denmark
Jiang, Liudi, University of Southampton, UK
Jiang, Wei, University of Virginia, USA
Jiao, Zheng, Shanghai University, China
John, Joachim, IMEC, Belgium
Kalach, Andrew, Voronezh Institute of Ministry of Interior, Russia
Kang, Moonho, Sunmoon University, Korea South
Kaniusas, Eugenijus, Vienna University of Technology, Austria
Katake, Anup, Texas A&M University, USA
Kausel, Wilfried, University of Music, Vienna, Austria
Kavasoglu, Nese, Mugla University, Turkey
Ke, Cathy, Tyndall National Institute, Ireland
Khan, Asif, Aligarh Muslim University, Aligarh, India
Sapozhnikova, Ksenia, D.I.Mendeleyev Institute for Metrology, Russia

Kim, Min Young, Kyungpook National University, Korea South
Ko, Sang Choon, Electronics and Telecommunications Research Institute, Korea South
Kockar, Hakan, Balikesir University, Turkey
Kotulska, Malgorzata, Wroclaw University of Technology, Poland
Kratz, Henrik, Uppsala University, Sweden
Kumar, Arun, University of South Florida, USA
Kumar, Subodh, National Physical Laboratory, India
Kung, Chih-Hsien, Chang-Jung Christian University, Taiwan
Lacnjevac, Caslav, University of Belgrade, Serbia
Lay-Ekuakille, Aime, University of Lecce, Italy
Lee, Jang Myung, Pusan National University, Korea South
Lee, Jun Su, Amkor Technology, Inc. South Korea
Lei, Hua, National Starch and Chemical Company, USA
Li, Genxi, Nanjing University, China
Li, Hui, Shanghai Jiaotong University, China
Li, Xian-Fang, Central South University, China
Liang, Yuanchang, University of Washington, USA
Liawruangrath, Saisunee, Chiang Mai University, Thailand
Liew, Kim Meow, City University of Hong Kong, Hong Kong
Lin, Hermann, National Kaohsiung University, Taiwan
Lin, Paul, Cleveland State University, USA
Linderholm, Pontus, EPFL - Microsystems Laboratory, Switzerland
Liu, Aihua, University of Oklahoma, USA
Liu Changgeng, Louisiana State University, USA
Liu, Cheng-Hsien, National Tsing Hua University, Taiwan
Liu, Songqin, Southeast University, China
Lodeiro, Carlos, Universidade NOVA de Lisboa, Portugal
Lorenzo, Maria Encarnacio, Universidad Autonoma de Madrid, Spain
Lukaszewicz, Jerzy Pawel, Nicholas Copernicus University, Poland
Ma, Zhanfang, Northeast Normal University, China
Majstorovic, Vidosav, University of Belgrade, Serbia
Marquez, Alfredo, Centro de Investigacion en Materiales Avanzados, Mexico
Matay, Ladislav, Slovak Academy of Sciences, Slovakia
Mathur, Prafull, National Physical Laboratory, India
Maurya, D.K., Institute of Materials Research and Engineering, Singapore
Mekid, Samir, University of Manchester, UK
Melnyk, Ivan, Photon Control Inc., Canada
Mendes, Paulo, University of Minho, Portugal
Mennell, Julie, Northumbria University, UK
Mi, Bin, Boston Scientific Corporation, USA
Minas, Graca, University of Minho, Portugal
Moghavvemi, Mahmoud, University of Malaya, Malaysia
Mohammadi, Mohammad-Reza, University of Cambridge, UK
Molina Flores, Esteban, Benemérita Universidad Autónoma de Puebla, Mexico
Moradi, Majid, University of Kerman, Iran
Morello, Rosario, University "Mediterranea" of Reggio Calabria, Italy
Mounir, Ben Ali, University of Sousse, Tunisia
Mulla, Imtiaz Sirajuddin, National Chemical Laboratory, Pune, India
Neelamegam, Periasamy, Sastra Deemed University, India
Neshkova, Milka, Bulgarian Academy of Sciences, Bulgaria
Oberhammer, Joachim, Royal Institute of Technology, Sweden
Ould Lahoucine, Cherif, University of Guelma, Algeria
Pamidighanta, Sayanu, Bharat Electronics Limited (BEL), India
Pan, Jisheng, Institute of Materials Research & Engineering, Singapore
Park, Joon-Shik, Korea Electronics Technology Institute, Korea South
Penza, Michele, ENEA C.R., Italy
Pereira, Jose Miguel, Instituto Politecnico de Setebal, Portugal
Petsev, Dimiter, University of New Mexico, USA
Pogacnik, Lea, University of Ljubljana, Slovenia
Post, Michael, National Research Council, Canada
Prance, Robert, University of Sussex, UK
Prasad, Ambika, Gulbarga University, India
Prateepasen, Asa, Kingmoungut's University of Technology, Thailand
Pullini, Daniele, Centro Ricerche FIAT, Italy
Pumera, Martin, National Institute for Materials Science, Japan
Radhakrishnan, S. National Chemical Laboratory, Pune, India
Rajanna, K., Indian Institute of Science, India
Ramadan, Qasem, Institute of Microelectronics, Singapore
Rao, Basuthkar, Tata Inst. of Fundamental Research, India
Raoof, Kosai, Joseph Fourier University of Grenoble, France
Reig, Candid, University of Valencia, Spain
Restivo, Maria Teresa, University of Porto, Portugal
Robert, Michel, University Henri Poincare, France
Rezazadeh, Ghader, Urmia University, Iran
Royo, Santiago, Universitat Politecnica de Catalunya, Spain
Rodriguez, Angel, Universidad Politecnica de Cataluna, Spain
Rothberg, Steve, Loughborough University, UK
Sadana, Ajit, University of Mississippi, USA
Sadeghian Marnani, Hamed, TU Delft, The Netherlands
Sandacci, Serghei, Sensor Technology Ltd., UK
Saxena, Vibha, Bhbha Atomic Research Centre, Mumbai, India
Schneider, John K., Ultra-Scan Corporation, USA
Seif, Selemani, Alabama A & M University, USA
Seifter, Achim, Los Alamos National Laboratory, USA
Sengupta, Deepak, Advance Bio-Photonics, India
Shearwood, Christopher, Nanyang Technological University, Singapore
Shin, Kyuho, Samsung Advanced Institute of Technology, Korea
Shmaliy, Yuriy, Kharkiv National Univ. of Radio Electronics, Ukraine
Silva Girao, Pedro, Technical University of Lisbon, Portugal
Singh, V. R., National Physical Laboratory, India
Slomovitz, Daniel, UTE, Uruguay
Smith, Martin, Open University, UK
Soleymanpour, Ahmad, Damghan Basic Science University, Iran
Somani, Prakash R., Centre for Materials for Electronics Technol., India
Srinivas, Talabattula, Indian Institute of Science, Bangalore, India
Srivastava, Arvind K., Northwestern University, USA
Stefan-van Staden, Raluca-Ioana, University of Pretoria, South Africa
Sumriddetchka, Sarun, National Electronics and Computer Technology Center, Thailand
Sun, Chengliang, Polytechnic University, Hong-Kong
Sun, Dongming, Jilin University, China
Sun, Junhua, Beijing University of Aeronautics and Astronautics, China
Sun, Zhiqiang, Central South University, China
Suri, C. Raman, Institute of Microbial Technology, India
Sysoev, Victor, Saratov State Technical University, Russia
Szewczyk, Roman, Industrial Research Inst. for Automation and Measurement, Poland
Tan, Ooi Kiang, Nanyang Technological University, Singapore,
Tang, Dianping, Southwest University, China
Tang, Jaw-Luen, National Chung Cheng University, Taiwan
Teker, Kasif, Frostburg State University, USA
Thumbavanam Pad, Kartik, Carnegie Mellon University, USA
Tian, Gui Yun, University of Newcastle, UK
Tsiantos, Vassilios, Technological Educational Institute of Kaval, Greece
Tsigara, Anna, National Hellenic Research Foundation, Greece
Twomey, Karen, University College Cork, Ireland
Valente, Antonio, University, Vila Real, - U.T.A.D., Portugal
Vaseashta, Ashok, Marshall University, USA
Vazquez, Carmen, Carlos III University in Madrid, Spain
Vieira, Manuela, Instituto Superior de Engenharia de Lisboa, Portugal
Vigna, Benedetto, STMicroelectronics, Italy
Vrba, Radimir, Brno University of Technology, Czech Republic
Wandelt, Barbara, Technical University of Lodz, Poland
Wang, Jiangping, Xi'an Shiyou University, China
Wang, Kedong, Beihang University, China
Wang, Liang, Advanced Micro Devices, USA
Wang, Mi, University of Leeds, UK
Wang, Shinn-Fwu, Ching Yun University, Taiwan
Wang, Wei-Chih, University of Washington, USA
Wang, Wensheng, University of Pennsylvania, USA
Watson, Steven, Center for NanoSpace Technologies Inc., USA
Weiping, Yan, Dalian University of Technology, China
Wells, Stephen, Southern Company Services, USA
Wolkenberg, Andrzej, Institute of Electron Technology, Poland
Woods, R. Clive, Louisiana State University, USA
Wu, DerHo, National Pingtung Univ. of Science and Technology, Taiwan
Wu, Zhaoyang, Hunan University, China
Xiu Tao, Ge, Chuzhou University, China
Xu, Lisheng, The Chinese University of Hong Kong, Hong Kong
Xu, Tao, University of California, Irvine, USA
Yang, Dongfang, National Research Council, Canada
Yang, Wuqiang, The University of Manchester, UK
Yang, Xiaoling, University of Georgia, Athens, GA, USA
Yaping Dan, Harvard University, USA
Ymeti, Aurel, University of Twente, Netherland
Yong Zhao, Northeastern University, China
Yu, Haihu, Wuhan University of Technology, China
Yuan, Yong, Massey University, New Zealand
Yufera Garcia, Alberto, Seville University, Spain
Zagnoni, Michele, University of Southampton, UK
Zamani, Cyrus, Universitat de Barcelona, Spain
Zeni, Luigi, Second University of Naples, Italy
Zhang, Minglong, Shanghai University, China
Zhang, Qintao, University of California at Berkeley, USA
Zhang, Weiping, Shanghai Jiao Tong University, China
Zhang, Wenming, Shanghai Jiao Tong University, China
Zhang, Xueji, World Precision Instruments, Inc., USA
Zhong, Haoxiang, Henan Normal University, China
Zhu, Qing, Fujifilm Dimatix, Inc., USA
Zorzano, Luis, Universidad de La Rioja, Spain
Zourob, Mohammed, University of Cambridge, UK

Sensors & Transducers Journal (ISSN 1726-5479) is a peer review international journal published monthly online by International Frequency Sensor Association (IFSA).
Available in electronic and on CD. Copyright © 2009 by International Frequency Sensor Association. All rights reserved.

Sensors & Transducers Journal

Contents

Volume 6
Special Issue
August 2009

www.sensorsportal.com

ISSN 1726-5479

Research Articles

Authors are encouraged to submit article in MS Word (doc) and Acrobat (pdf) formats by e-mail: editor@sensorsportal.com
Please visit journal's webpage with preparation instructions: http://www.sensorsportal.com/HTML/DIGEST/Submition.htm

International Frequency Sensor Association (IFSA).

Sensors & Transducers Journal, Vol. 6, Special Issue, August 2009, pp. 43-56

Sensors & Transducers

ISSN 1726-5479

http://www.sensorsportal.com

Estimation of Back-Surface Flaw Depth by Laminated Piezoelectric Highpolymer Film

Akinobu YAMAMOTO, Shiro BIWA and Eiji MATSUMOTO
Department of Energy Conversion Science,
Graduate School of Energy Science, Kyoto University
Kyoto, 606-8501, Japan
Tel./fax: +81-(0)75-753-5247
E-mail: matumoto@energy.kyoto-u.ac.jp

Received: 10 July 2009 /Accepted: 31 July 2009 /Published: 10 August 2009

Abstract: Piezoelectric thin films have been used to visualize back surface flaws in plates. If the plate with a surface flaw is deformed, the strain distribution appears on the other surface reflecting the location and the shape of the flaw. Such surface strain distribution can be transformed into the electric potential distribution on the piezoelectric film mounted on the plate surface. This paper deals with a NDE technique to estimate the depth of a back-surface flaw from the electric potential distribution on a laminated piezoelectric thin film. It is experimentally verified that the flaw depth can be exactly estimated by the peak height of the electric potential distribution. *Copyright © 2009 IFSA.*

Keywords: piezoelectricity, polyvinylidene fluoride (PVDF), NDE, flaw detection, sizing technique

---

1. Introduction

Conventional nondestructive evaluation (NDE) techniques for flaw detection utilize instruments which transmit/receive some kinds of energies into/from the objects. In order to inspect a region of the object, we should scan the probe or the direction of the energy emission by an additional mechanism. In order to estimate the shape or the size of a flaw, some kind of signal processing of receiving data is required. On the other hand, flaw inspection technique using mounted piezoelectric thin film enables us to inspect a region of the object without emitting energies into the object. Piezoelectric material induces the electric voltage when it is deformed. When a material with a flaw is subjected to the stress, the strain distribution occurs around the flaw. If we attach a piezoelectric thin film onto the surface of a plate, the strain distribution generated by the flaw can be measured from the potential distribution on the film even in the case of a back-surface flaw. Egashira et al [1] measured the local strains in notched plates in tension from the potential distribution of mounted polyvinylidene fluoride (PVDF) film. Matsumoto et al [2] have shown that the location and the apertural shape of a back surface flaw can be identified by PVDF film attached onto the plate. Chishiki et al [3] achieved the isotropic sensitivity and inspection ability of the film by laminating two PVDF films.

For effective maintenance of the structural safety, lifetime prognostic is important as well as diagnosis of the structural health. Exact prognostic requires the sizing of flaws more than their detection. Among nondestructive sizing techniques proposed up to now, ultrasonic techniques have been most widely used because of their reliability and practicality [4]. On the other hand, other NDE techniques are also expected to be applied to the sizing of flaws which cover shortcomings of the ultrasonic techniques [5, 6].

From the above back ground, this paper considers the sizing of the flaws by NDE techniques using PVDF film. That is, we try to estimate the depth of a back-surface flaw from the electric potential distribution on laminated PVDF film. We prepare a thicker film for high sensitivity and laminate two films for isotropic sensitivity. In order to obtain the reference data for the depth estimation, we numerically calculate the potential distributions on the laminated film for various depths of flaws. The potential distribution on the film along a line takes a peak at the back position of a flaw, which can be approximated by an elementally function. From the simulated result, we shall present an evaluation formula to estimate the flaw depth from a parameter of the approximated potential distribution. It is verified that the estimated depths of artificial flaws are in good agreement with the actual ones.

2. Relation of Electric Potential and Strain of PVDF Film

Throughout the paper we assume that the deformation of the specimen and the piezoelectricity of the PVDF film are not large within the ranges of linear responses. According to [7] and [8], the linear constitutive equations of piezoelectric materials are given by

$$\begin{aligned} \boldsymbol{D} &= \boldsymbol{eS} + \varepsilon\boldsymbol{E} \\ \boldsymbol{T} &= \boldsymbol{cS} - \boldsymbol{e}^T \boldsymbol{E} \end{aligned}, \tag{1}$$

where D is the electric displacement, E the electric field, S the strain tensor, T the stress tensor, ε the electric permeability tensor at fixed S, c the elastic coefficient tensor at fixed E, and e the piezoelectric coefficient tensor of third order. Henceforth symmetric tensors of the second order such as S and T are expressed in Voigt notation, i.e., the independent components of a symmetric tensor are expressed as a vector of the six-dimensional space by replacing indices as (11)→(1), (22)→(2), (33)→(3), (23)→(4), (31)→(5) and (12)→(6).

Let coordinates x_1 and x_2 lie on the film surface and x_1 axis coincide with the rolling direction of the film. One surface of the film is covered by an electrode layer and no true charge exists in the film. When the film is deformed, from the Maxwell equations and the above conditions we have $D_3=0$, $E_1=E_2=0$. Since the film is sufficiently thin (30 or 40 μm), we can assume that the out-of-plane stress in the film vanishes; $T_3= T_4 =T_5=0$. Substituting the above conditions into the constitutive equations (1), we obtain

$$\begin{aligned} 0 &= \sum_{i=1}^{3} e_{3i} S_i + \varepsilon_{33} E_3 \\ 0 &= \sum_{i=1}^{3} c_{3i} S_i - e_{33} E_3 \end{aligned}. \tag{2}$$

Eliminating S_3 in the above equations and rearranging the result by use of the electromechanical coupling constant k_t , we have,

$$\begin{aligned} 0 &= \left(e_{31} - \frac{c_{31}}{c_{33}} e_{33} \right) S_1 + \left(e_{32} - \frac{c_{32}}{c_{33}} e_{33} \right) S_2 + \varepsilon_{33} \left(1 + k_t^{\,2} \right) E_3 \\ &= e'_{31} S_1 + e'_{32} S_2 + \varepsilon_{33} (1 + k_t^2) E_3 \end{aligned} . \tag{3}$$

Equation (3) can be solved for E_3 as

$$E_3 = -\frac{1}{\varepsilon_{33} (1 + k_t^{\,2})} \left(e'_{31}\, S_1 + e'_{32}\, S_2 \right) . \tag{4}$$

Here we have put

$$e'_{3k} = e_{3k} - \left(c_{3k} / c_{33} \right) e_{33} \quad \left(k = 1,2 \right) . \tag{5}$$

Let d denote the thickness of the film and suppose that the electrode surface of the film is grounded. Then from (4) the voltage on the film surface can be expressed in terms of the plane strain components at each point of the film [9].

$$V = -dE_3 = \frac{d}{\varepsilon_{33} \left(1 + k_t^{\,2} \right)} \left(e'_{31} S_1 + e'_{32} S_2 \right) . \tag{6}$$

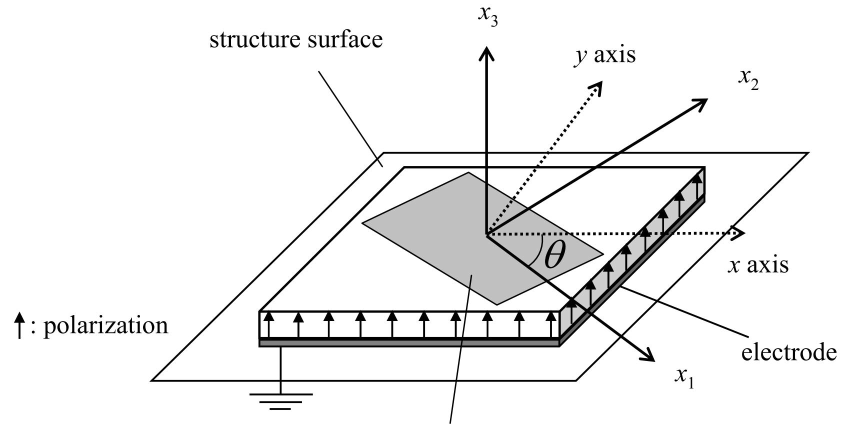

Fig. 1. Coordinate systems in PVDF film and structure.

We next consider that the PVDF film is attached to the plane surface of a structural material by insulate adhesive. Since the film is thin and the rigidity of PVDF film is very small compared with the structural material, the plane strain components at each point of the film coincide with the surface strain components at the same point of the object. Let alternate coordinate axes x and y be set on the object surface and θ denote the angle between x_1 and x axes of two coordinate systems, respectively, in the film and the object. Then the strain components S_1 and S_2 in the coordinate axes x_1 and x_2 are expressed in terms of the strain components S_x, S_y and S_{xy} in the coordinate axes x and y as

$$\begin{aligned} S_1 &= S_x \cos^2\theta + S_y \sin^2\theta + 2S_{xy}\sin\theta\cos\theta \\ S_2 &= S_x \sin^2\theta + S_y \cos^2\theta - 2S_{xy}\sin\theta\cos\theta \end{aligned} . \tag{7}$$

Substituting the above equations into (6), we have

$$V(\theta) = \frac{d}{\varepsilon_{33}\left(1+k_t^{\,2}\right)}\left\{\left(e'_{31}\cos^2\theta + e'_{32}\sin^2\theta\right)S_x + \left(e'_{31}\sin^2\theta + e'_{32}\cos^2\theta\right)S_y + \left(e'_{31} - e'_{32}\right)S_{xy}\sin 2\theta\right. . \tag{8}$$

In general, the right hand side of the above equation depends on the angle θ. In special cases θ=0° and θ=90°, the contribution of the shear strain vanishes in (8) to yield

$$V(0°) = p_1 S_x + p_2 S_y \tag{9}$$

$$V(90°) = p_2 S_x + p_1 S_y \ . \tag{10}$$

Here coefficients p_1 and p_2 are given by

$$p_1 = \frac{de'_{31}}{\varepsilon_{33}(1+k_t^2)},\ p_2 = \frac{de'_{32}}{\varepsilon_{33}(1+k_t^2)}\ , \tag{11}$$

refer to [9]. Thus, in these special cases the shear stress component does not influence to the induced voltage of the film. We next consider a laminated film and derive the relation between the induced voltage on the film and the strain components. We attach a single layer film on the object surface in a similar manner to the previous discussion and laminate another film without electrode layer onto the original film. The voltage on the top surface of the laminated film is given by the sum of the voltages of two films at each point. If the polarization directions of both films are the same and the rolling directions of both films make angle 90°, the voltage on the top surface of the laminated film is given by replacing θ with θ+90° in (8) and add the result to (8):

$$V(\theta) = V(\theta) + V\left(\theta + 90^\circ\right) = \left(p_1 + p_2\right)\left(S_x + S_y\right)\ , \tag{12}$$

which implies that the induced voltage of the above laminated film does not depend on the angle θ. In other words, the distribution of the electric potential on the film surface does not depend on the mounting direction of the film. This prediction was experimentally verified by Hashimura et al [10]. It is also seen from (12) that the induced voltage is proportional to the sum of the principal plane strain components. Note that the induced voltage on the surface of a single or a laminated film depends on the local strain at each point of the object, so that the potential distribution on the film surface corresponds to the surface strain distribution of the object.

3. Determination of Coefficients in Strain-Voltage Relation

Coefficients p_1 and p_2 in (11) can be determined by the uniaxial tension test for a specimen mounted on PVDF film. That is, we attach a film onto an acrylic specimen and apply the uniaxial stress parallel or perpendicular to the rolling direction. We have used PVDF films with 30 μm thickness in the previous studies, but the sensitivity of PVDF film should be improved for precise qualitative estimation of flaw size. Thus in this paper we use another commercial PVDF films with 40 μm thickness. In view of (11), coefficients p_1 and p_2 are proportional to the film thickness if the material properties are the same.

However the effects of rolling and poling during processing to the film properties may be different for 30 μm and 40 μm thicknesses, so that we measure the above coefficients for PVDF films with both thicknesses by tension test along x_1 and x_2 axes of the coordinates system in the film.

We also verify that the coefficients p_1 and p_2, that is, the sensitivity of PVDF film does not depend on the characteristic of the object material mounted on PVDF film. In experimental verification of NDE technique by PVDF film, high polymer material acrylic has been used as the object material from the following reason. The strain inversely depends on the elastic coefficients of the object material for the same geometrical condition and the same applied stress. In fact, acrylic has low rigidity compared with metals and hence large strain distribution or large potential distribution is caused by flaws, which is convenient for experimental verification. The NDE technique by PVDF film utilizes the localized deformation of the object around flaws under the stress, whose estimated result does not depend on other material properties except the mechanical ones. However if the conductor is used as the object material in place of the insulator, influence of the electric condition by the conductor to the PVDF film should be considered. So we measure coefficients p_1 and p_2 for PVDF films with 40μm thickness attached to aluminum strip as well as those for acrylic strip.

3.1. Measurement Method

We attached two PVDF films onto an acrylic and aluminum strips such that x_1 axis of the film is parallel or perpendicular to the tension direction. Here the Young's modulus and the Poison's ratio of acrylic are 3.4GPa and 0.39, and those of aluminium are 70.3GPa and 0.345, respectively. Similarly to the precious section, the contact side of the film to the specimen has a grounded electrode layer and we apply a uniaxial tension to the specimen with three different strain rates. The strain of the strip is measured by the strain gauge and the induced voltage on the film surface is measured by the electrostatic voltmeter. Substituting the measured strain S_x and the voltage into (9) and (10), we obtain simultaneous equations for coefficients p_1 and p_2.

3.2. Determination of Coefficients

Fig. 2 and Fig. 3 show the induced voltage on PVDF films onto an aluminum strip at each strain when the uniaxial stress is applied along x_1 and x_2 axes, respectively. From the figures we see that the induced voltages linearly depend on the strain but not on the strain rates. We also see that the induced voltages of the thicker film are larger than those of the thinner film. We obtain the slopes of the voltage-strain curves in Fig. 2 and Fig. 3 by the least square method, which equal to the coefficients of S_x in (9) and (10). The corresponding transverse strain S_y is given by $-\nu S_x$ for the uniaxial stress. Substituting the obtained strains into (9) and (10) and solving the equations for p_1 and p_2, we have coefficients p_1 and p_2 given by Table 1. As expected, PVDF film with 40 μm thickness has larger coefficients p_1 and p_2, but they are not exactly proportional to the thickness. This may come from the difference in film processing. In fact, the piezoelectric constants provided by the film producer are different for two types of films. In general, coefficient p_1 is larger than p_2 from the effect of the anisotropy induced by rolling process of the film, whose ratio drastically changes with the rolling ratio [11]. In order to improve the sensitivity of the film we shall employ the film with 40 μm thickness in what follows.

Fig. 4 and Fig. 5 show the induced voltage on PVDF films with 40 μm thickness onto an acrylic strip at each strain when the uniaxial stress is applied along x_1 and x_2 axes, respectively. From the figures we see that the induced voltages linearly depend on the strain but not on the strain rates as well as Fig. 2 and Fig. 3 Similarly to the case of aluminum strip, we obtain coefficients p_1 and p_2 as shown in Table 2 for the film with 40 μm thickness. It is found that both coefficients of the PVDF films with 40 μm thickness onto an acrylic and an aluminum strips are approximately equal.

Table. 1 Measured coefficients.

PVDF thickness	p_1[V]	p_2[V]
30 μm	1.90×10^4	9.81×10^3
40 μm	3.19×10^4	1.63×10^4

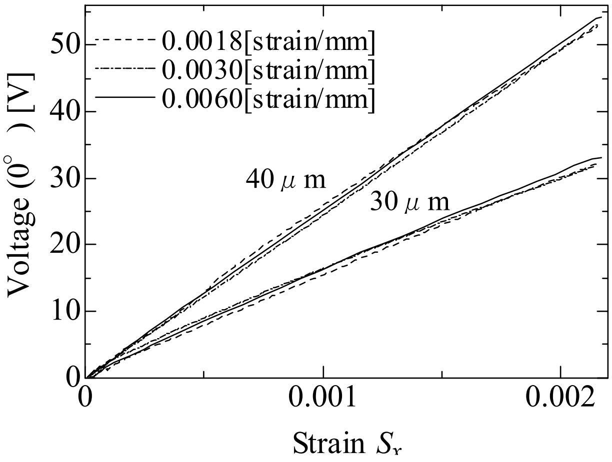

Fig. 2. Relation between voltage and strain (x_1 axis). (Aluminum).

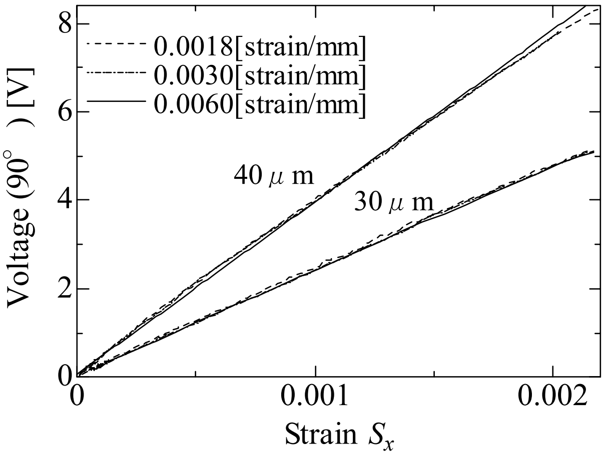

Fig. 3. Relation between voltage and strain (x_2 axis). (Aluminum).

Table. 2 Measured coefficients.

Specimen	p_1[V]	p_2[V]
Aluminum	3.07×10^4	1.68×10^4
Acrylic	3.19×10^4	1.63×10^4

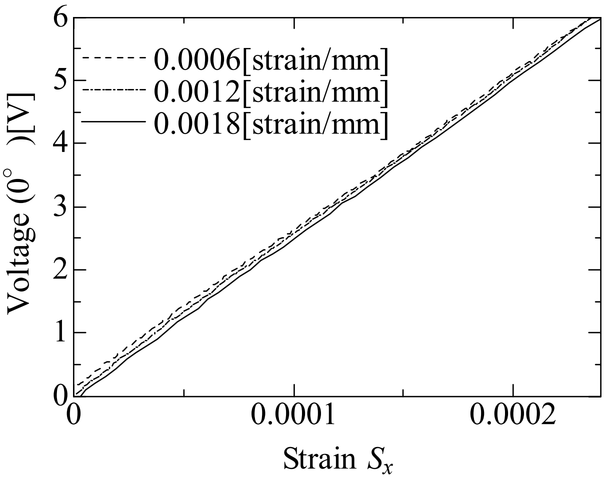

Fig. 4. Relation between voltage and strain (x_1 axis). (Acrylic).

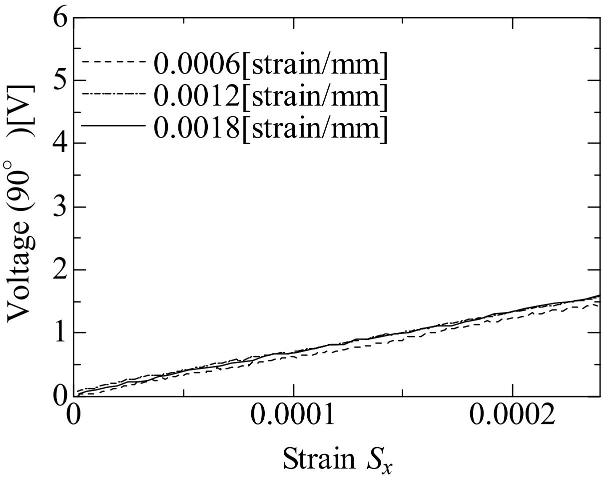

Fig. 5. Relation between voltage and strain (x_2 axis). (Acrylic).

4. Estimation of Back-Surface Flaw Depth by Laminated PVDF Film

4.1. Simulation for Deriving Estimation Formula of Flaw Depth

In order to drive the estimation formula of flaw depth, we analyze the relation of the flaw depth and the electrical potential distribution on the laminated PVDF film by means of numerical simulation. In simulation, we use high polymer material acrylic as the object material. The size of the acrylic specimen is 70 mm length, 50 mm width and 10mm thickness. For each calculation, an artificial slit-like flaw with 12 mm length is installed in the center of the specimen surface, see Fig. 6. The depths of installed flaws are from 1 mm to 9 mm with 1mm increment, and the widths from 1 mm to 3 mm with 1mm increment. From the geometrical symmetry, a quarter region of the specimen is divided by tetra meshes. Compressive stress is applied in the direction as shown in Fig. 6 such that −0.1 % strain is induced in the smooth region far from the flaw. The deformation of the specimen under the above conditions is analyzed by FEM software ANSYS. The electric potential distribution on the surface of PVDF film is obtained by substituting the calculated surface strain into (12).

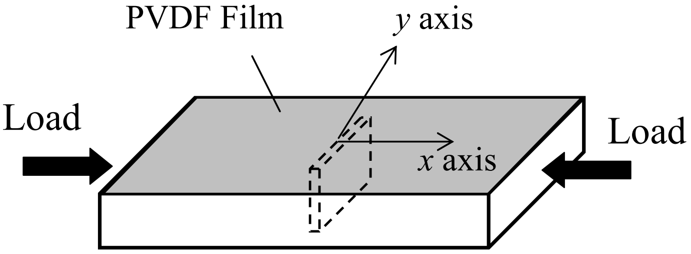

Fig. 6. Simulation Model.

4.2. Characteristic Parameters of Potential Distribution Induced by Back-Surface Flaw

As an example of the simulated results discussed in the previous subsection, Fig. 7 shows the planar potential distribution on the laminated PVDF film in case of the flaw with 12 mm length and 5 mm depth. In view of Fig. 7, the maximum voltage appears at the center of the flaw area on the film, and the aperture shape of the flaw can be inferred by the pattern of the potential distribution. On the other hand, the voltage at distant points from the flaw is around −30 V, which is caused by the bias −0.1% strain and the pyroelectricity of PVDF film. In Fig. 7 the minimum voltage appears both sides of the flaw and a steep peak of the potential appears at the center of the flaw. Fig. 8 shows the distribution of the electric potential at line y=0. The heap shape of the electric potential may reflect the cross section of the flaw at y=0. Fig. 9 shows the relation of the flaw depth and the peak height of the potential, which implies that the peak height linearly depends on the flaw depth in the range smaller than 7mm (70 % of the specimen thickness). The linear dependence becomes the same line for the flaw widths between 1mm and 3mm. In a practical life estimation of structural materials based on NDE, it is important to estimate smaller flaw depths compared with the structure thickness. Thus, we shall derive an estimation formula for flaw depth smaller than 7mm. Differently from the simulated data, experimentally obtained electric potential distribution may not be smooth from the measurement errors like Fig. 8. In order to extract characteristic parameters from such experimental distributions, we approximate the distribution of the electric potential at y=0 in the form

$$V = A\exp\left\{-B(x-D)^2\right\}+C. \tag{13}$$

Here V denotes the voltage, A the height of the potential peak, B the sharpness of the peak, C the bias potential induced by the applied compressive strain and the pyroelectric effect of PVDF, and D the location of the flaw on the line y=0. In Fig. 10 we show the approximated potential distribution at line y=0 on the laminated PVDF film obtained from the simulated distributions.

In the next subsection we present an evaluation formula for the flaw depth by use of parameter A.

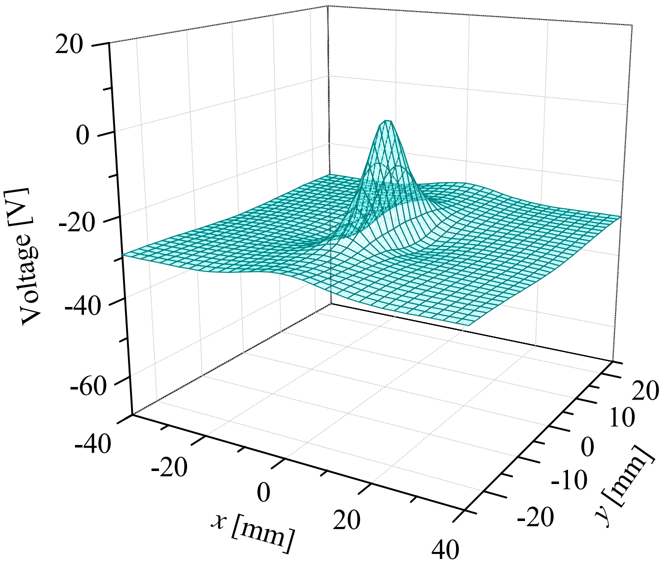

Fig. 7. Planar distribution of electric potential on PVDF film.

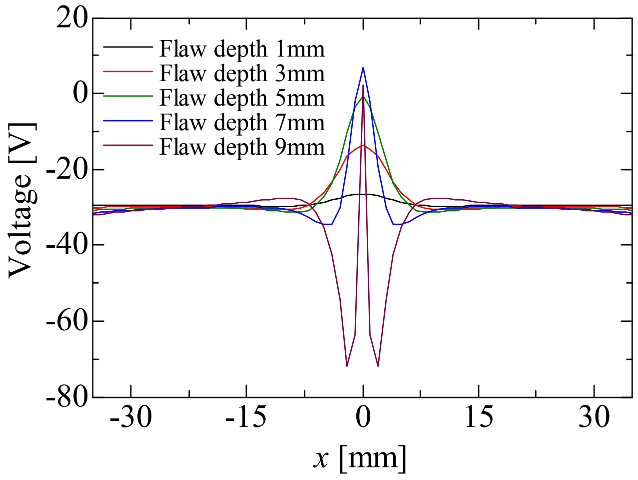

Fig. 8. Distribution of electric potential on PVDF film.

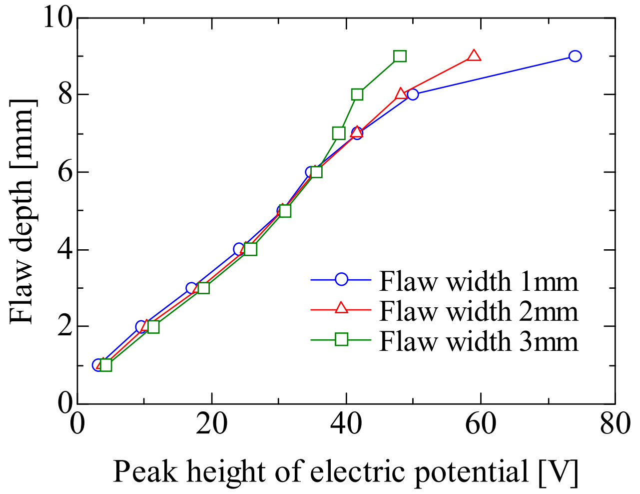

Fig. 9. Dependence of potential peak on flaw depth.

4.3. Evaluation Formula for Flaw Depth

From Fig. 10, we obtain the relation of the flaw depth and the parameter A in the range of the flaw depth smaller than 7mm as shown in Fig. 11. Fig. 11 shows that parameter A linearly depends on the flaw depth for each width as well as Fig. 9. By the least square method the linear dependence can be expressed as

$$F_d = 0.173A \quad \text{for} \quad -0.1\% \ \text{strain} . \tag{14}$$

Here F_d is the estimated flaw depth. Since the relation between the flaw depth and the potential height may depend on the bias strain, we also obtain the linear curves for bias strains –0.05% and –0.2%, see Fig. 12 and Fig. 13.

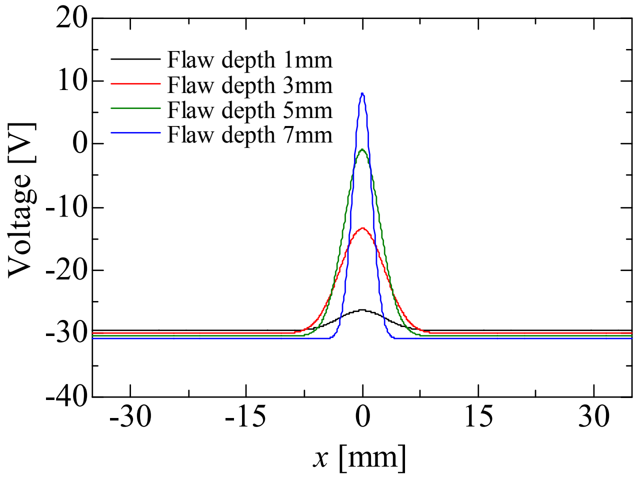

Fig. 10. Approximated distribution of electric potential. (1 mm flaw width).

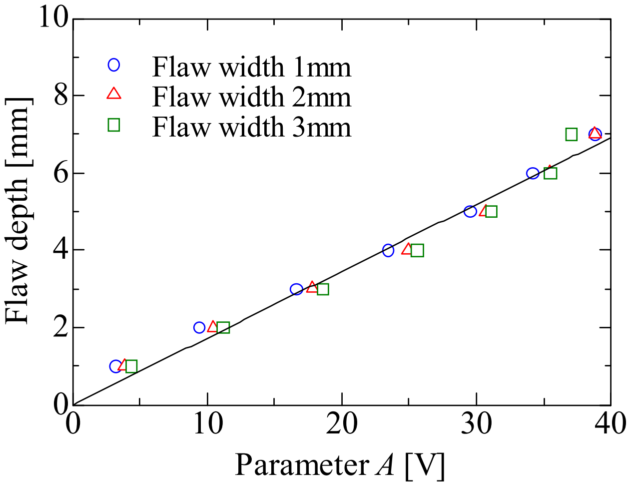

Fig. 11. Dependence of parameter A on flaw depth. (0.1 % strain).

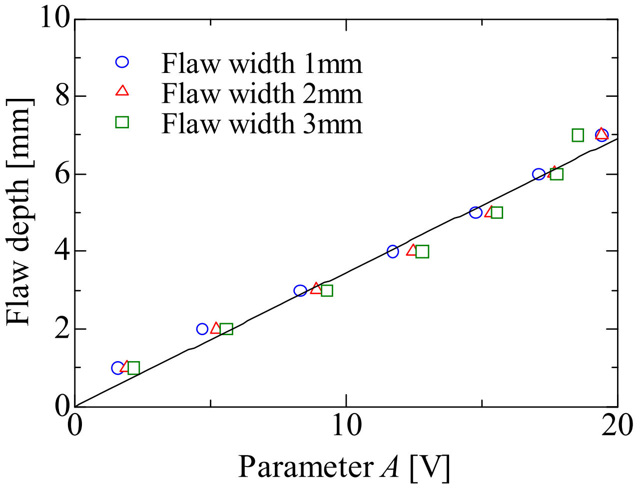

Fig. 12. Dependence of parameter A on flaw depth. (0.05 % strain).

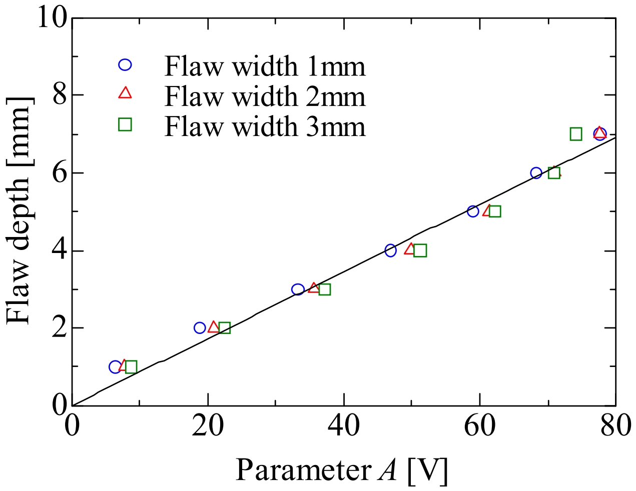

Fig. 13. Dependence of parameter A on flaw depth. (0.2 % strain).

$$F_d = 0.346A \text{ for } -0.05\ \% \text{ strain,} \tag{15}$$

$$F_d = 0.087A \text{ for } -0.2\ \% \text{ strain .} \tag{16}$$

We see that all the plots in Fig. 11, Fig. 12 and Fig. 13 locate on a similar linear curve, if we neglect the difference in the ranges of the horizontal axes. Since the mechanical deformation of the object and the piezoelectric behavior of PVDF can be regarded as small enough for linear response, the induced voltage and hence the potential height A may be proportional to the bias strain for each flaw size. In fact, three linear curves (14)-(16) can be expressed in a single linear curve if we normalize the height of the induced potential peak A by the bias strain S as

$$F_d = 1.73 \times 10^{-4} \frac{A}{S} . \tag{17}$$

It should be noted that the formula (17) can be applied to flaws whose depths are smaller than 7 mm and widths are between 1 mm and 3 mm. In the next subsection, we shall attempt to estimate unknown depth of flaws by the formula (17).

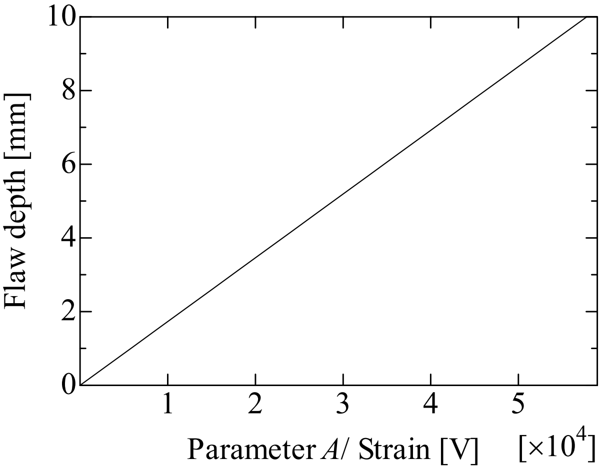

Fig. 14. Relation between flaw depth and parameter *A* / strain.

4.4. Estimation of Unknown Flaw Depth.

Fig. 15 shows the experimental setup for estimation of flaw depths in acrylic specimens by the proposed method.

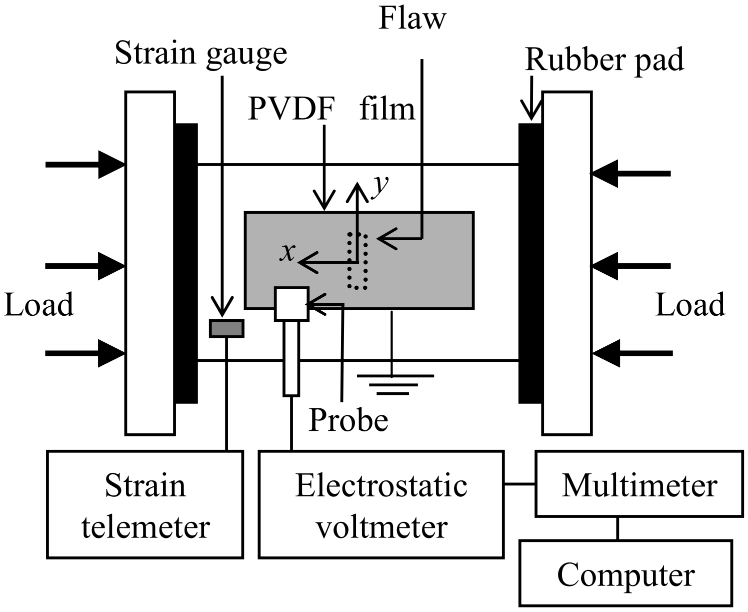

Fig. 15. Experimental setup.

We prepare three specimens I, П and Ш with flaws, whose lengths are 12 mm and cross sectional sizes are given in Table 3. We attach a laminated PVDF film with 40×2 μm thickness on the center of the specimen surface by epoxy resin adhesive such that the electrode layer contacts with the specimen surface. We apply 0.05 % and 0.1 % compressions to specimens I and П in a similar way to the simulation and 0.1 % and 0.2 % compressions to specimen Ш. We measure the electric potential along line y=0 on the PVDF film by 1.0 mm intervals. We start to measure the potential several minutes after applying the stress, by taking into account the creep deformation of the high polymer material. We also measure the electric potential before applying the stress, and take the difference of the potentials at each point of PVDF film to cancel the effect of the pyroelectricity. Furthermore, the potential distribution on PVDF film is relaxed in some extent during several hours. Thus we finish the measurement of the potential distribution in the shortest possible time such that the time variation of the potential distribution can be neglected.

From Fig. 16 to Fig. 21 we show the measured potential distributions at line y=0, approximated potential distributions by (13), and the simulated distributions. According to the discussions in the previous subsection, we determine parameter A as Table 4 to Table 6. Then from parameter A and each bias strain, we can estimate the flaw depth by use of (17) as Table 7 to Table 9, which implies that the unknown flaw depths can be estimated precisely by the proposed formula. In these tables, parameter D indicates the position of each flaw center at line y=0, which are around less than ±1 mm. Since we have set the origin of the coordinate axis at each flaw center, the proposed method can estimate the location of each flaw within 1mm error. In these tables, we can see the differences in the parameters for the simulated and the experimental potential distributions. The differences may come from the effects of the pyroelectricity, the relaxation of the piezoelectricity, the deformation of acrylic specimens, etc. Evaluation of such influences is left for future subject. In spite of the differences in other parameters, parameter A is not influenced so much by these effects, and the relative accuracy of estimation of flaw depth increases as the bias strain or the flaw depth increases.

Table 3. Flaw sizes of prepared specimens.

	width [mm]	depth [mm]
Specimen I	1.0	1.0
SpecimenП	2.5	3.5
Specimen Ш	3.0	7.0

Table 4. Parameters for specimen I.

Specimen I	Simulation	Experiment
Parameter A (0.05 %)	1.61	2.50
Parameter B (0.05 %)	0.055	0.034
Parameter C (0.05 %)	-14.77	-15.06
Parameter D (0.05 %)	0	1.15
Parameter A (0.1 %)	3.21	4.36
Parameter B (0.1 %)	0.055	0.044
Parameter C (0.1 %)	-29.53	-28.85
Parameter D (0.1 %)	0	-0.03

Table 5. Parameters for specimen П.

Specimen П	Simulation	Experiment
Parameter *A* (0.05 %)	10.97	10.76
Parameter *B* (0.05 %)	0.056	0.047
Parameter *C* (0.05 %)	-15.15	-16.15
Parameter *D* (0.05 %)	0	0.38
Parameter *A* (0.1 %)	21.94	20.05
Parameter *B* (0.1 %)	0.056	0.039
Parameter *C* (0.1 %)	-30.29	-31.28
Parameter *D* (0.1 %)	0	0.35

Table 6. Parameters for specimen Ш.

Specimen Ш	Simulation	Experiment
Parameter *A* (0.1 %)	37.08	40.5
Parameter *B* (0.1 %)	0.21	0.11
Parameter *C* (0.1 %)	-31.09	-36.35
Parameter *D* (0.1 %)	0	0.024
Parameter *A* (0.2 %)	74.16	80.87
Parameter *B* (0.2 %)	0.21	0.10
Parameter *C* (0.2 %)	-62.19	-73.86
Parameter *D* (0.2 %)	0	-0.33

Table 7. Exact and estimated flaw depths for specimen I.

Specimen I	Flaw depth [mm]	Estimated depth [mm]
0.05 % Strain	1.0	0.86
0.1 % Strain	1.0	0.76

Table 8. Exact and estimated flaw depths for specimen П.

Specimen Ⅱ	Flaw depth [mm]	Estimated depth [mm]
0.05 % Strain	3.5	3.72
0.1 % Strain	3.5	3.47

Table 9. Exact and estimated flaw depths for specimen Ш.

SpecimenⅢ	Flaw depth [mm]	Estimated depth [mm]
0.1 % Strain	7.0	7.01
0.2 % Strain	7.0	7

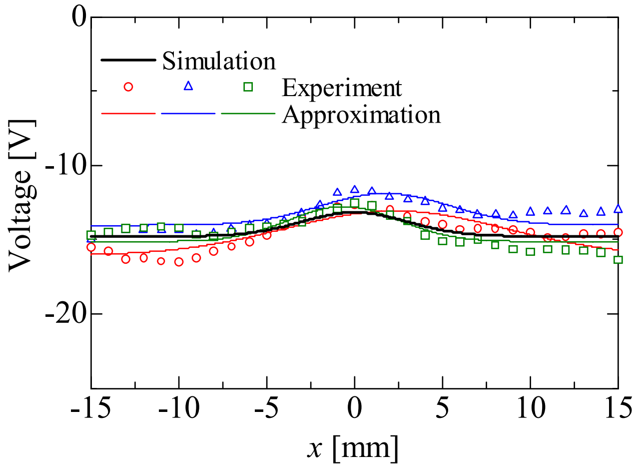

Fig. 16. Distribution of electric potential for 0.05 % strain. (Specimen I).

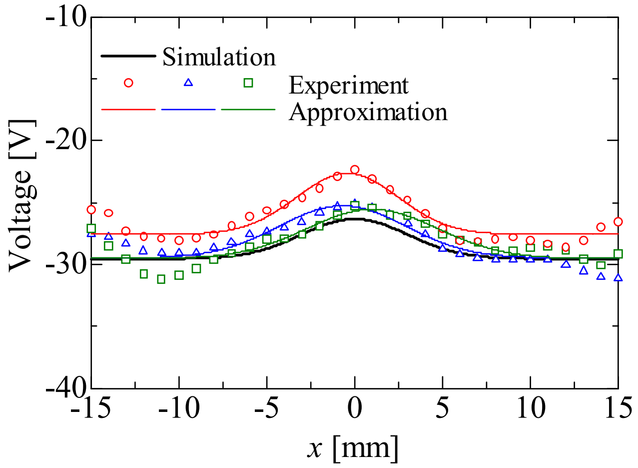

Fig. 17. Distribution of electric potential for 0.1 % strain. (Specimen I).

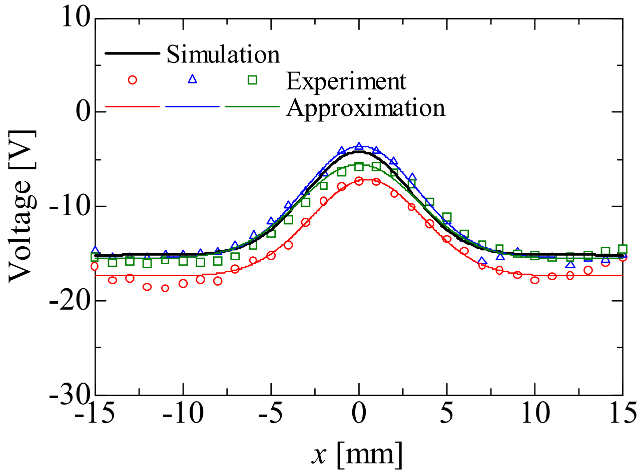

Fig. 18. Distribution of electric potential for 0.05 % strain. (Specimen Ⅱ).

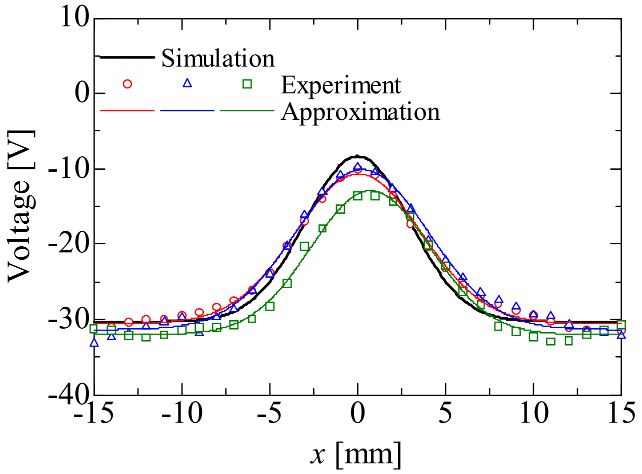

Fig. 19. Distribution of electric potential for 0.1 % strain. (Specimen Ⅱ).

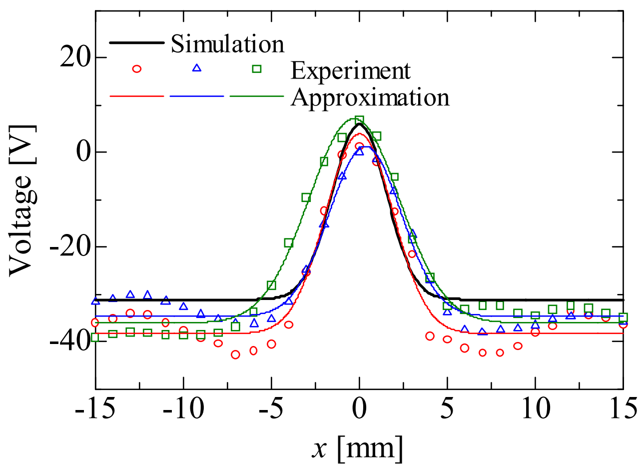

Fig. 20. Distribution of electric potential for 0.1 % strain. (Specimen Ⅲ).

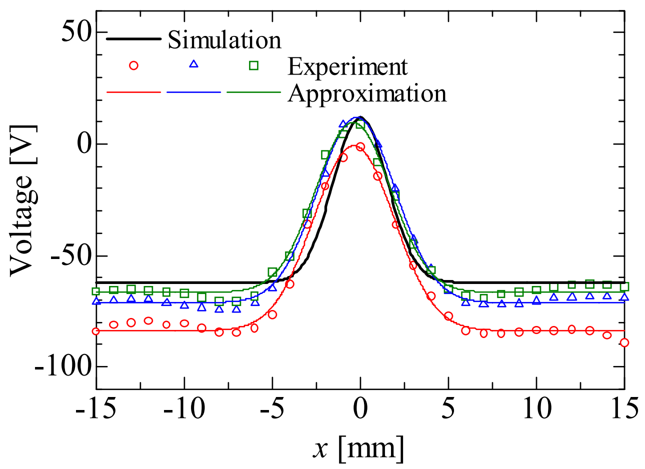

Fig. 21. Distribution of electric potential for 0.2 % strain. (Specimen Ⅲ).

5. Conclusions

This paper attempts to evaluate the size of flaw depth by the laminated piezoelectric high polymer (PVDF) film. The obtained results are as follows.

1. The sensitivity of PVDF film is improved by making the film thicker and laminating two films.
2. From numerical simulation, obtained are the correlation with the flaw depth and the parameter characterizing the height of the potential distribution on a laminated PVDF film. When the flaw depth is smaller than 70 % of the specimen thickness, the relation of the flaw depth and the height of the potential peak becomes linear curve without depending on the flaw width for each bias strain.
3. We have derived the estimation formula of the flaw depth which follows for any bias strain by normalizing the induced electric potential.
4. The proposed sizing technique for flaw depth is verified by the experiment. It is found that the flaw depth can be precisely estimated by measuring the electric potential distribution along a line crossing the flaw center.

References

[1]. M. Egashira, N. Shinya, Local Strain Sensing Using Piezoelectric Polymer, *Journal of Intelligent Material Systems and Structures*, Vol. 4, 1993, pp. 558-560.

[2]. K. Katsumi, S. Biwa, E. Matsumoto and T. Shibata, Measurement of Static Strain Distribution Using Piezoelectric Polymer Film (Principle and Application to a Holed Plate), *JSME International Journal A*, Vol. 64, No. 617, 1998, pp. 215-220.

[3]. J. Chishiki, Y. Komagome, E. Matsumoto, Detection of back surface defect by laminated piezoelectric polymer film, *Journal of the Japan Society of Applied Electromagnetics and Mechanics*, Vol. 10, No. 4, 2002, pp. 372-377.

[4]. S. Lin, H. Fukutomi, and T. Ogata, Development of New Flaw Depth Sizing Technique in Ultrasonic Testing, Part 5, *Journal of the Japan Society of Mechanical Engineers*, Vol. 74, No. 738, 2008, pp. 185-190.

[5]. Abe Masataka, Biwa Shiro, Eiji Matsumoto, 3D Shape Identification of Perpendicular Flaw by Biaxial MFLT with Neural Network, in *Proceedings of the Conference on Toward Innovative Nuclear Safety and Simulation Technology (ISSNP'2008)*, 8-10 September 2008, Vol. 1, pp. 106-112.

[6]. Akinobu Yamamoto, Shiro Biwa, Eiji Matsumoto, Sizing of Back-Surface Flaws by Piezoelectric Highpolymer Film, in *Proceedings of the 3rd International Conference on Sensing Technology(ICST'2008)*, Tainan, 30 November-3 December, IEEE Catalog Number CFP0818E-CDR, ISBN987-1-4244-2177-0, Paper ID: 96.

[7]. Horie, Taniguchi, Electro-Optics Functional Organic Material Handbook, *Asakura Publishing Co., Ltd.,* 1995, p. 613.

[8]. Advanced materials series, Ferroelectricity and high-Tc superconductivity, The Society of Materials Science, *Shokabo Publishing Co., Ltd*., 1993.

[9]. S. Biwa, K. Katsumi, Y. Omoto, E. Matsumoto and T. Shibata, Sensing Technique for Surface Strain Distribution with Piezoelectric Film, *J. Electrical Engineering,* Vol. 48, 8/S, 1997, pp. 50-53.

[10].T. Hashimura, E. Matsumoto, Detection of cracks and back surface defects by piezoelectric high-polymer film, *Journal of the Japan Society of Applied Electromagnetics and Mechanics*, Vol. 13. No. 1, 2005, pp. 50-55.

[11].S. Tanaka, S. Miyata, The origin of piezoelectricity in poly (vinylidene fluoride), *Ferroelectric*, 32, 1981, pp. 17-23.

Guide for Contributors

Aims and Scope

Sensors & Transducers Journal (ISSN 1726-5479) provides an advanced forum for the science and technology of physical, chemical sensors and biosensors. It publishes state-of-the-art reviews, regular research and application specific papers, short notes, letters to Editor and sensors related books reviews as well as academic, practical and commercial information of interest to its readership. Because it is an open access, peer review international journal, papers rapidly published in *Sensors & Transducers Journal* will receive a very high publicity. The journal is published monthly as twelve issues per annual by International Frequency Association (IFSA). In additional, some special sponsored and conference issues published annually. *Sensors & Transducers Journal* is indexed and abstracted very quickly by Chemical Abstracts, IndexCopernicus Journals Master List, Open J-Gate, Google Scholar, etc.

Topics Covered

Contributions are invited on all aspects of research, development and application of the science and technology of sensors, transducers and sensor instrumentations. Topics include, but are not restricted to:

- Physical, chemical and biosensors;
- Digital, frequency, period, duty-cycle, time interval, PWM, pulse number output sensors and transducers;
- Theory, principles, effects, design, standardization and modeling;
- Smart sensors and systems;
- Sensor instrumentation;
- Virtual instruments;
- Sensors interfaces, buses and networks;
- Signal processing;
- Frequency (period, duty-cycle)-to-digital converters, ADC;
- Technologies and materials;
- Nanosensors;
- Microsystems;
- Applications.

Submission of papers

Articles should be written in English. Authors are invited to submit by e-mail editor@sensorsportal.com 8-14 pages article (including abstract, illustrations (color or grayscale), photos and references) in both: MS Word (doc) and Acrobat (pdf) formats. Detailed preparation instructions, paper example and template of manuscript are available from the journal's webpage: http://www.sensorsportal.com/HTML/DIGEST/Submition.htm Authors must follow the instructions strictly when submitting their manuscripts.

Advertising Information

Advertising orders and enquires may be sent to sales@sensorsportal.com Please download also our media kit: http://www.sensorsportal.com/DOWNLOADS/Media_Kit_2009.pdf

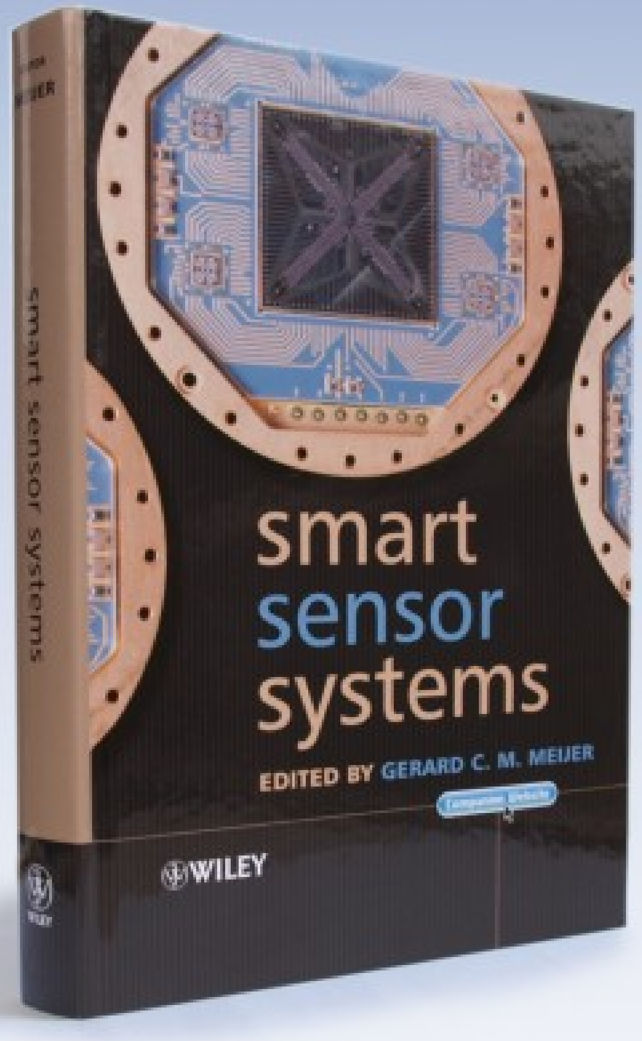

smart sensor systems
EDITED BY GERARD C. M. MEIJER
WILEY

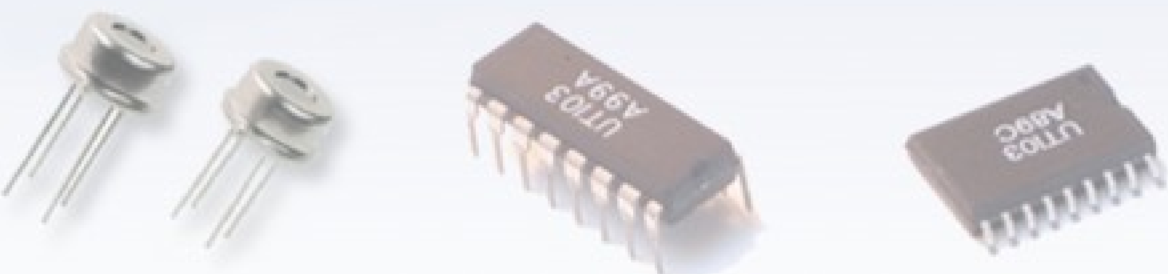

UT103
A99A
UT103
A88C